

Catalytic Decomposition of Hydrogen Peroxide by Fe(III) in Homogeneous Aqueous Solution: Mechanism and Kinetic Modeling

JOSEPH DE LAAT* AND HERVÉ GALLARD

Laboratoire de Chimie de l'Eau et de l'Environnement, CNRS UPRESA 6008, Ecole Supérieure d'Ingénieurs de Poitiers, Université de Poitiers, 40, avenue du Recteur Pineau, 86 022 Poitiers Cedex, France

This paper describes a kinetic model for the decomposition of hydrogen peroxide by ferric ion in homogeneous aqueous solution (pH < 3). The reaction was investigated experimentally at 25.0 °C and $I = 0.1$ M (HClO₄/NaClO₄), in a completely mixed batch reactor and under a wide range of experimental conditions ($1 \leq \text{pH} \leq 3$; $0.2 \text{ mM} \leq [\text{H}_2\text{O}_2]_0 \leq 1 \text{ M}$; $50 \mu\text{M} \leq [\text{Fe(III)}]_0 \leq 1 \text{ mM}$; $1 \leq [\text{H}_2\text{O}_2]_0 / [\text{Fe(III)}]_0 \leq 5000$). The results of this study demonstrated that the rate of decomposition of hydrogen peroxide by Fe(III) could be predicted very accurately by a kinetic model which takes into account the rapid formation and the slower decomposition of Fe(III)–hydroperoxy complexes (Fe^{III}(HO₂)²⁺ and Fe^{III}(OH)(HO₂)⁺). The rate constant for the unimolecular decomposition of the Fe(III)–hydroperoxy complexes was determined to be $2.7 \times 10^{-3} \text{ s}^{-1}$. The use of the kinetic model allows a better understanding of the effects of operational parameters (i.e., pH and $[\text{H}_2\text{O}_2]_0 / [\text{Fe(III)}]_0$) on the complex kinetics of decomposition of H₂O₂ by Fe(III).

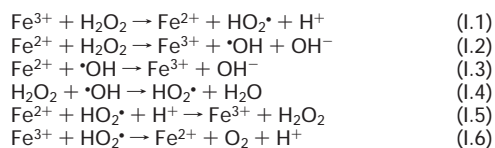
Introduction

The mechanism and kinetics of decomposition of hydrogen peroxide (H₂O₂) by Fe(II) and Fe(III) species have been the subject of numerous investigations over the last century (1–5). These reactions are of interest in biochemistry (6, 7) and in the chemistry of atmospheric water droplets (8, 9) and of natural waters (10). In water treatment, the use of advanced oxidation processes (AOPs), which involve the in-situ generation of highly reactive hydroxyl radicals (•OH), has emerged during the last two decades. The dark reaction of H₂O₂ with ferrous salts (known as Fenton's reagent) and the photo-assisted decomposition of H₂O₂ (Photo-Fenton) are possible sources of hydroxyl radicals for the destruction of organic pollutants (11–15).

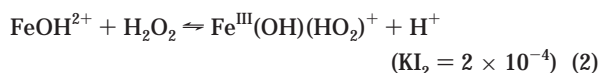
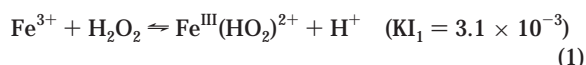
For the Fe(III)/H₂O₂ system, H₂O₂ is catalytically decomposed by Fe(III) at acidic pH. The reaction pathway accepted by most of the authors proceeds through the formation of hydroxyl and hydroperoxyl radicals (Table 1) (16, 17). For simplification, coordinated water molecules in the coordinate sphere are not presented in the chemical formulas.

Spectrophotometric studies have shown that the reaction of H₂O₂ with Fe³⁺ primarily leads to the formation of an Fe(III)–hydroperoxy complex formulated as Fe^{III}(HO₂)²⁺ (18). At very high concentrations of H₂O₂, the formation of diperoxo

TABLE 1. Mechanism of Decomposition of H₂O₂ by Fe³⁺ (16, 17)

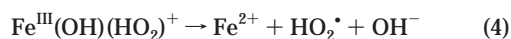
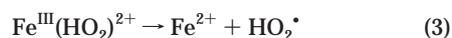


complexes has also been suggested (19–21). In a recent study carried out with ferric perchlorate in solution in perchloric acid between pH 1.0 and 3.0, our spectral data gave evidence for the formation of two Fe(III)–hydroperoxy complexes (22), formulated in their simplest forms as Fe^{III}(HO₂)²⁺ (I₁) and Fe^{III}(OH)(HO₂)⁺ (I₂):



The formation of these complexes is very fast and equilibria are attained within a few seconds after mixing of Fe(III) and H₂O₂ solutions. The equilibrium constants KI₁ and KI₂, determined at 25.0 (± 0.2) °C and $I = 0.1$ M (HClO₄/NaClO₄ solution) were estimated as 3.1×10^{-3} and 2×10^{-4} , respectively (22).

Once formed, the Fe(III)–hydroperoxy complexes are assumed to decompose in a unimolecular way to yield Fe²⁺ and HO₂• (16, 17):



The rates of decomposition of Fe(III)–peroxy complexes are not well-known. It has been estimated as $1.1 \times 10^{-2} \text{ s}^{-1}$ at 30 °C (23) by using $\text{KI}_1 = 3.65 \times 10^{-3}$ (18).

The rate of decomposition of H₂O₂ by Fe(III) has been studied extensively, and many kinetic models derived from hypothetical mechanisms have been tested (16, 17, 24). Nevertheless, no model describes well the overall rate of decomposition of H₂O₂ over a wide range of experimental conditions (pH, Fe(III), and H₂O₂ concentrations). Reasons for this might be the complexity of the decomposition pathway of H₂O₂ by Fe(III) and of the considerable uncertainties on the various equilibrium and kinetic constants of individual reactions. Furthermore, the formation of Fe(III)–hydroperoxy complexes as intermediates has never been considered in the kinetic models.

The objective of the present work is therefore to formulate an appropriate reaction model for the homogeneous catalytic decomposition of H₂O₂ by Fe(III) which takes into account the formation of Fe(III)–hydroperoxy complexes and to test its applicability for interpreting the overall rate of decomposition of H₂O₂ under various experimental conditions.

This study has been carried out with ferric perchlorate in perchloric acid/sodium perchlorate solution and in the absence of organic solutes. A future paper will describe a kinetic modeling for the oxidation of organic compounds by Fe(III)/H₂O₂.

Model Reaction and Kinetic Expressions

The kinetic model incorporates the reactions and their equilibrium or rate constants listed in Table 2. In the reaction model, the following reactions have been considered:

* Corresponding author phone: 33 5 49 45 39 21; fax: 33 5 49 45 37 68; e-mail: Joseph.DeLaat@esip.univ-poitiers.fr.

TABLE 2. Proposed Reaction Mechanism for Fe(III)-Catalyzed Decomposition of H₂O₂ (25 °C; I = 0.1 M)

no.	reactions	constants ^a	refs
(II.1)	Fe ³⁺ + H ₂ O ⇌ FeOH ²⁺ + H ⁺	K ₁ = 2.9 × 10 ⁻³ M	(25)
(II.2)	Fe ³⁺ + 2H ₂ O ⇌ Fe(OH) ₂ ⁺ + 2H ⁺	K ₂ = 7.62 × 10 ⁻⁷ M ²	(25)
(II.3)	2Fe ³⁺ + 2H ₂ O ⇌ Fe ₂ (OH) ₂ ⁴⁺ + 2H ⁺	K _{2,2} = 0.8 × 10 ⁻³ M	(26)
(II.4)	Fe ³⁺ + H ₂ O ₂ ⇌ Fe ^{III} (HO ₂) ²⁺ + H ⁺	KI ₁ = 3.1 × 10 ⁻³	(22)
(II.5)	FeOH ²⁺ + H ₂ O ₂ ⇌ Fe ^{III} (OH)(HO ₂) ⁺ + H ⁺	KI ₂ = 2.0 × 10 ⁻⁴	(22)
(II.6a)	Fe ^{III} (HO ₂) ²⁺ → Fe ²⁺ + HO ₂ [•]	k ₆ = 2.7 × 10 ⁻³ s ⁻¹	this study
(II.6b)	Fe ^{III} (OH)(HO ₂) ⁺ → Fe ²⁺ + HO ₂ [•] + OH ⁻	k ₆ = 2.7 × 10 ⁻³ s ⁻¹	this study
(II.7)	Fe ²⁺ + H ₂ O ₂ → Fe ³⁺ + •OH + OH ⁻	k ₇ = 63.0 ^a M ⁻¹ s ⁻¹	(27)
(II.8)	Fe ²⁺ + •OH → Fe ³⁺ + OH ⁻	k ₈ = 3.2 × 10 ⁸ M ⁻¹ s ⁻¹	(31)
(II.9)	•OH + H ₂ O ₂ → HO ₂ [•] + H ₂ O	k ₉ = 3.3 × 10 ⁷ M ⁻¹ s ⁻¹	(32)
(II.10a)	Fe ²⁺ + HO ₂ [•] → Fe ^{III} (HO ₂) ²⁺	k _{10a} = 1.2 × 10 ⁶ M ⁻¹ s ⁻¹	(33)
(II.10b)	Fe ²⁺ + O ₂ ^{-•} + H ⁺ → Fe ^{III} (HO ₂) ²⁺	k _{10b} = 1.0 × 10 ⁷ M ⁻¹ s ⁻¹	(34)
(II.11a)	Fe(III) + HO ₂ [•] → Fe ²⁺ + O ₂ + H ⁺	k _{11a} < 2 × 10 ³ M ⁻¹ s ⁻¹	(34)
(II.11b)	Fe(III) + O ₂ ^{-•} → Fe ²⁺ + O ₂	k _{11b} = 5 × 10 ⁷ M ⁻¹ s ⁻¹	(35)
(II.12a)	HO ₂ [•] → O ₂ ^{-•} + H ⁺	k _{12a} = 1.58 × 10 ⁵ s ⁻¹	(36)
(II.12b)	O ₂ ^{-•} + H ⁺ → HO ₂ [•]	k _{12b} = 1 × 10 ¹⁰ M ⁻¹ s ⁻¹	(36)
(II.13a)	HO ₂ [•] + HO ₂ [•] → H ₂ O ₂ + O ₂	k _{13a} = 8.3 × 10 ⁵ M ⁻¹ s ⁻¹	(36)
(II.13b)	HO ₂ [•] + O ₂ ^{-•} + H ₂ O → H ₂ O ₂ + O ₂ + OH ⁻	k _{13b} = 9.7 × 10 ⁷ M ⁻¹ s ⁻¹	(36)
(II.14a)	•OH + HO ₂ [•] → H ₂ O + O ₂	k _{14a} = 0.71 × 10 ¹⁰ M ⁻¹ s ⁻¹	(37)
(II.14b)	•OH + O ₂ ^{-•} → OH ⁻ + O ₂	k _{14b} = 1.01 × 10 ¹⁰ M ⁻¹ s ⁻¹	(37)
(II.15)	•OH + •OH → H ₂ O ₂	k ₁₅ = 5.2 × 10 ⁹ M ⁻¹ s ⁻¹	(37)

^a Apparent second-order rate constant for the reaction of H₂O₂ with Fe(II) at pH < 3.5.

(1) The hydrolysis of Fe(III) (reactions II.1–II.3 in Table 2): Equilibrium constants for Fe(III) hydrolysis used in this study were calculated for 0.1 M ionic strength from literature values (25, 26).

(2) The initiation step: The initiation step of the mechanism of decomposition of H₂O₂ by Fe(III) includes the formation of the Fe(III)–hydroperoxy complexes (reactions II.4 and II.5) and their unimolecular decomposition which yields Fe²⁺ and HO₂[•]/O₂^{-•} (reactions II.6a and II.6b). The equilibrium constants (KI₁, KI₂) for the formation of Fe^{III}(HO₂)²⁺ (I₁) and Fe^{III}(OH)(HO₂)⁺ (I₂) have been determined in a previous work (22) conducted at 25 °C and I = 0.1 M.

(3) The propagation and termination steps represented by reactions II.7–II.12b: For the reaction between Fe(II) and H₂O₂ (reaction II.7, Table 2), a previous study (27) carried out with ferrous perchlorate in HClO₄/NaClO₄ solutions (25 °C; I = 0.1 M) has shown that the decomposition of H₂O₂ by Fe(II) ([Fe(II)]₀/[H₂O₂]₀ > 2) proceeds through the formation of two intermediates which might be an Fe(III)–hydroperoxy complex and the ferryl ion (28–30). At pH < 3.5 and in the presence of very low concentrations of organic compounds (< 2 μM), our kinetic results gave evidence that overall reaction II.7 in Table 2 (with k₇ = 63 M⁻¹ s⁻¹) could be used to describe the rate of the initiation step of the decomposition mechanism of H₂O₂ by Fe(II) and the rate of production of OH radical.

(4) Recombination of radicals (reactions II.13a–II.15) which may represent minor pathways have also been considered.

For calculations, the following assumptions and simplifications have been made:

(1) Complexation reactions of Fe(III) and acid–base equilibrium were considered to be very fast equilibrium processes.

(2) The rate constants for the unimolecular decomposition of I₁ and I₂, which are unknown, are assumed to be identical and equal to k₆. It should be noted that under our experimental conditions (pH < 3.5), I₁ is the predominant Fe(III)–hydroperoxy complex.

(3) The Fe(III)–hydroperoxy complexes I₁ and I₂ do not participate in propagation and termination reactions. Therefore, it has been assumed that only uncomplexed Fe(III) participates in these reactions (reactions II.11a and II.11b).

According to the reaction scheme presented in Table 2, the concentration–time profiles for H₂O₂, Fe²⁺, Fe(III), and for radical species can be described by the following set of differential equations:

$$d[\text{Fe}^{2+}]/dt = k_6(I_1 + I_2) - k_7[\text{Fe}^{2+}][\text{H}_2\text{O}_2] - k_8[\text{Fe}^{2+}][\text{•OH}] - k_{10a}[\text{Fe}^{2+}][\text{HO}_2^{\bullet}] - k_{10b}[\text{Fe}^{2+}][\text{O}_2^{\bullet-}] + k_{11a}[\text{Fe(III)}][\text{HO}_2^{\bullet}] + k_{11b}[\text{Fe(III)}][\text{O}_2^{\bullet-}] \quad (5)$$

$$d[\text{Fe(III)}]_T/dt = -d[\text{Fe}^{2+}]/dt \quad (6)$$

$$d[\text{H}_2\text{O}_2]/dt = -k_7[\text{Fe}^{2+}][\text{H}_2\text{O}_2] - k_9[\text{H}_2\text{O}_2][\text{•OH}] + k_{13a}[\text{HO}_2^{\bullet}][\text{HO}_2^{\bullet}] + k_{13b}[\text{O}_2^{\bullet-}][\text{HO}_2^{\bullet}] + k_{15}[\text{•OH}][\text{•OH}] \quad (7)$$

$$d[\text{•OH}]/dt = k_7[\text{Fe}^{2+}][\text{H}_2\text{O}_2] - k_8[\text{Fe}^{2+}][\text{•OH}] - k_9[\text{H}_2\text{O}_2][\text{•OH}] - k_{14a}[\text{•OH}][\text{HO}_2^{\bullet}] - k_{14b}[\text{•OH}][\text{O}_2^{\bullet-}] - 2k_{15}[\text{•OH}][\text{•OH}] \quad (8)$$

$$d[\text{HO}_2^{\bullet}]/dt = k_6(I_1 + I_2) + k_9[\text{H}_2\text{O}_2][\text{•OH}] - k_{10a}[\text{Fe}^{2+}][\text{HO}_2^{\bullet}] - k_{11a}[\text{Fe(III)}][\text{HO}_2^{\bullet}] - k_{12a}[\text{HO}_2^{\bullet}] + k_{12b}[\text{O}_2^{\bullet-}][\text{H}^+] - 2k_{13a}[\text{HO}_2^{\bullet}][\text{HO}_2^{\bullet}] - k_{13b}[\text{O}_2^{\bullet-}][\text{HO}_2^{\bullet}] - k_{14a}[\text{•OH}][\text{HO}_2^{\bullet}] \quad (9)$$

$$d[\text{O}_2^{\bullet-}]/dt = -k_{10b}[\text{Fe}^{2+}][\text{O}_2^{\bullet-}] - k_{11b}[\text{Fe(III)}][\text{O}_2^{\bullet-}] + k_{12a}[\text{HO}_2^{\bullet}] - k_{12b}[\text{O}_2^{\bullet-}][\text{H}^+] - k_{13b}[\text{O}_2^{\bullet-}][\text{HO}_2^{\bullet}] - k_{14b}[\text{•OH}][\text{O}_2^{\bullet-}] \quad (10)$$

where [Fe(III)]_T and [Fe(III)] are the total concentration of Fe(III) and the concentration of uncomplexed Fe(III), respectively:

$$[\text{Fe(III)}]_T = [\text{Fe(III)}] + [I_1] + [I_2] \quad (11)$$

$$[\text{Fe(III)}] = [\text{Fe}^{3+}] + [\text{FeOH}^{2+}] + [\text{Fe(OH)}_2^+ + 2[\text{Fe}_2(\text{OH})_2^{4+}] \quad (12)$$

The system of nonlinear ordinary equations (eqs 5–10) was solved numerically on compatible PC (Turbo Pascal by Borland) by using the fourth-order Runge–Kutta method.

Steady-state conditions were assumed for the rate of radical species. The reaction parameters (pH, $[H_2O_2]_0$, $[Fe(III)]_0$) were specified as inputs to the program. Reaction rates and equilibrium constants, presented in Table 2, were also used as inputs to the program. The concentration–time profiles for H_2O_2 , Fe^{2+} , HO_2^*/O_2^{*-} , and $\cdot OH$ were calculated by the program, and the concentration of H_2O_2 predicted by the model was compared to the experimental measurements.

Experimental Section

All reagents used were reagent grade and were used without further purification. Ferric perchlorate ($Fe(ClO_4)_3 \cdot 9H_2O$, 98%) was purchased from Aldrich and hydrogen peroxide (30%, unstabilized) from Fluka. Stock solutions of H_2O_2 and ferric salts were prepared in ultrapure water (MilliQ water; $TOC \leq 0.2 \text{ mg L}^{-1}$; $18 \text{ } \Omega\text{cm}$).

Great care was taken to make ferric solutions to prevent precipitation of ferric hydroxide: an appropriate weight of $Fe(ClO_4)_3 \cdot 9H_2O$ was diluted in some milliliters of perchloric acid (0.1 N) and then added to an appropriate volume of ultrapure water to give the desired pH and concentration of $Fe(III)$. The ionic strength was adjusted to 0.1 M with sodium perchlorate (corresponding activity coefficient of H^+ equal to 0.85). Solutions of ferric salts were prepared daily, and kinetic experiments were rapidly carried out to prevent the effect of the maturation of monomeric $Fe(III)$ species to polymeric $Fe(III)$ species.

All experiments were conducted in a thermostated batch reactor ($25.0 \pm 0.2 \text{ } ^\circ\text{C}$) and in the absence of light. Kinetic experiments of the decomposition of H_2O_2 were initiated by adding H_2O_2 under vigorous magnetic-stirring to the solution containing ferric salt. At various intervals, samples of solution in the batch reactor were withdrawn during kinetic experiments and analyzed for H_2O_2 content.

Absorption spectra of the solutions were measured with a Safas DES 190 double beam spectrophotometer, and pH measurements were made with a Radiometer pH-meter (Model PHM 250) calibrated at $25 \text{ } ^\circ\text{C}$ with acidic standard buffers between pH 1.0 and 3.0.

Analysis of $Fe(II)$ was carried out by using *o*-phenanthroline colorimetric method (38) and using a value of $\epsilon = 11 \text{ } 300 \text{ M}^{-1} \text{ cm}^{-1}$ for the $Fe(II)$ –phenanthroline complex at 510 nm. Dissolved $Fe(III)$ concentrations were also measured by the *o*-phenanthroline method after filtration of the solution through a Millipore Millex-25 ($0.45 \text{ } \mu\text{M}$) filter and reduction of $Fe(III)$ into $Fe(II)$ with hydroxylamine hydrochlorate.

Hydrogen peroxide was determined iodometrically ($[H_2O_2] > 10^{-3} \text{ M}$) or spectrophotometrically using $TiCl_4$ method (39) ($[H_2O_2] \leq 10^{-3} \text{ M}$; $\epsilon = 730 \text{ M}^{-1} \text{ cm}^{-1}$). No interferences have been noticed with the concentrations of ferric ions used.

Results

For all the experiments performed in the present work, the initial rate of decomposition of H_2O_2 could be described by a pseudo-first-order kinetic law with respect to H_2O_2 concentration

$$\ln([H_2O_2]/[H_2O_2]_0) = -k_{obs}t \quad (13)$$

where k_{obs} is the pseudo-first-order rate constant of the initial rate of decomposition of H_2O_2 . k_{obs} was calculated from experimental data, covering 0–20% removal of H_2O_2 . The measured values for k_{obs} are reported in Tables 3 and 4. In experiments carried out in duplicate, k_{obs} varied by less than 3%.

Furthermore, pH was nearly constant during the course of the reaction (pH variation: <0.02 pH unit for experiments conducted at $pH \leq 2$, and ≤ 0.05 pH unit at $pH = 3$), and $Fe(II)$ analyses by the *o*-phenanthroline method revealed that $Fe(II)$ concentration was always less than $1 \text{ } \mu\text{M}$.

TABLE 3. Pseudo-First-Order Constants (k_{obs}) for the Initial Rate of the Decomposition of H_2O_2 by $Fe(III)$ at Different pH Values ($[Fe(III)]_0 = 200 \text{ } \mu\text{M}$; $[H_2O_2]_0 = 10 \text{ mM}$; $25 \text{ } ^\circ\text{C}$; $I = 0.1 \text{ M}$)

exp no.	pH	$k_{obs} (\times 10^6 \text{ s}^{-1})$	dissolved $[Fe(III)] (\mu\text{M})$
1	1.0	1.38	200
2	1.55	6.20	200
3	2.10	23.6	200
4	2.64	60.0	200
5	3.00	89.3	200
6	3.18	93.0	≈ 200
7	3.25	29.6	≈ 150
8	3.40	17.4	≈ 50
9	5.00	13.0	≈ 1

TABLE 4. Measured Pseudo-First-Order Kinetic Constants (k_{obs}) for the Initial Rate of Decomposition of H_2O_2 by $Fe(III)$ at pH 3.0 ($25 \text{ } ^\circ\text{C}$; $I = 0.1 \text{ M}$)

exp no.	$[Fe(III)]_0 (\mu\text{M})$	$[H_2O_2]_0 (\text{mM})$	$[H_2O_2]_0/[Fe(III)]_0$	$k_{obs} (\times 10^6 \text{ s}^{-1})$
1	50	2	40	19.3
2	50	50	1000	18.4
3	100	50	500	47.7
4	200	2	10	74.4
5	300	2	6.67	95.1
6	500	50	100	230.0
7	650	2	3.08	166.6
8	1000	2	2	212.0
9	1000	100	100	421.0
10	200	0.2	1	31.6
11	200	1	5	60.6
12	200	10	50	88.4
13	200	50	250	92.2
14	200	100	500	95.7
15	200	500	2500	75.5
16	200	955	4775	56.3

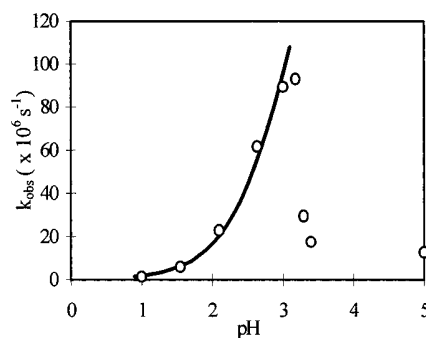


FIGURE 1. Effect of pH on the pseudo-first-order kinetic constant (k_{obs}) for the initial rate of decomposition of H_2O_2 by $Fe(III)$ (computed values (solid lines); experimental data (symbols); $[Fe(III)]_0 = 200 \text{ } \mu\text{M}$; $[H_2O_2]_0 = 10 \text{ mM}$; $25.0 \text{ } ^\circ\text{C}$; $I = 0.1 \text{ M}$).

Effect of pH on k_{obs} . Kinetic data obtained from experiments conducted at pH varying from 1.0 to 5.0 and with $[H_2O_2]_0/[Fe(III)]_0 = 50$ (Table 3, Figure 1) show that k_{obs} increases with pH in the range 1–3.2. Above pH 3.2, k_{obs} decreased with increasing pH. This decrease can be attributed to the precipitation of $Fe(III)$, as confirmed by the measured values obtained for dissolved $Fe(III)$ concentrations (Table 3).

Effect of $[H_2O_2]_0/[Fe(III)]_0$ on k_{obs} at pH 3.0. At constant pH (pH 3.0, Table 4), k_{obs} varied with the initial concentrations of reactants. For a constant initial concentration of $Fe(III)$ ($[Fe(III)]_0 = 200 \text{ } \mu\text{M}$), Figure 2 demonstrates the effect of the ratio of the initial concentration of H_2O_2 to $Fe(III)$ ($[H_2O_2]_0/$

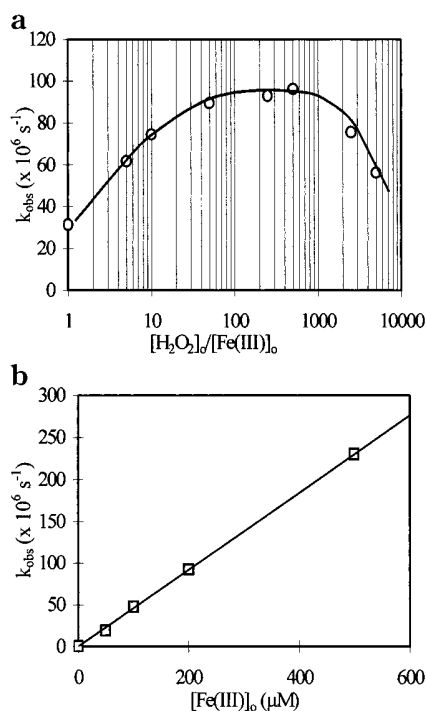


FIGURE 2. Effect of $[\text{H}_2\text{O}_2]_0$ and $[\text{Fe(III)}]_0$ on the pseudo-first-order kinetic constant (k_{obs}) for the initial rate of decomposition of H_2O_2 by Fe(III) at $\text{pH} = 3.0$ (computed values (solid lines); experimental data (symbols); 25.0°C ; $I = 0.1\text{ M}$): (a) effect of $[\text{H}_2\text{O}_2]_0$, $[\text{Fe(III)}]_0 = 200\ \mu\text{M}$ and (b) effect of $[\text{Fe(III)}]_0$, $[\text{H}_2\text{O}_2]_0 = 50\ \text{mM}$.

$[\text{Fe(III)}]_0$ on k_{obs} . For $[\text{H}_2\text{O}_2]_0/[\text{Fe(III)}]_0 < 50$, k_{obs} increased with increasing $[\text{H}_2\text{O}_2]_0/[\text{Fe(III)}]_0$. For $50 < [\text{H}_2\text{O}_2]_0/[\text{Fe(III)}]_0 < 500$, k_{obs} was nearly independent of $[\text{H}_2\text{O}_2]_0$ (at constant $[\text{Fe(III)}]_0$, Figure 2a) and increased linearly with $[\text{Fe(III)}]_0$ (Figure 2b). Under these conditions, a second-order kinetic law described the initial rate of decomposition of H_2O_2

$$-\text{d}[\text{H}_2\text{O}_2]/\text{d}t = k_d[\text{H}_2\text{O}_2][\text{Fe(III)}] \quad (14)$$

where k_d is the second-order rate constant for the overall rate of decomposition of H_2O_2 by Fe(III) . k_d was found to be equal to $0.47 (\pm 0.03)\ \text{M}^{-1}\ \text{s}^{-1}$ at $\text{pH} 3.0$ ($I = 0.1\ \text{M}$; 25°C). For $[\text{H}_2\text{O}_2]_0/[\text{Fe(III)}]_0 > 500$, k_{obs} decreased with increasing $[\text{H}_2\text{O}_2]_0/[\text{Fe(III)}]_0$. As will be discussed below, this decrease of k_{obs} was attributed to a decrease of the molar fraction of uncomplexed Fe(III) with increasing H_2O_2 concentration.

During the course of the reaction, the rate of decomposition of H_2O_2 deviates from the first-order kinetic law. The logarithm of $[\text{H}_2\text{O}_2]/[\text{H}_2\text{O}_2]_0$ plotted versus time did not follow a straight line but showed distinct curvature (Figure 3).

Kinetic Modeling. To test the reaction model proposed in Table 2, the kinetic model was run by varying the value of k_6 until a good fit between experimental data and model calculation was achieved. The best fit was obtained with $k_6 = 2.7 \times 10^{-3}\ \text{s}^{-1}$ for all the experiments performed at $\text{pH} < 3.2$. As shown in Figure 3, an excellent agreement between measured and simulated H_2O_2 concentration profiles versus reaction time was obtained.

In addition, the pseudo-first-order rate constants (k_{obs}) calculated from the initial slopes of simulated plots of $\ln([\text{H}_2\text{O}_2]/[\text{H}_2\text{O}_2]_0)$ versus time were consistent with the measured k_{obs} values for all the experiments conducted at $\text{pH} < 3.2$ (Figure 1). Above $\text{pH} 3.2$, the kinetic model cannot be applied since precipitation reactions of Fe(III) and their

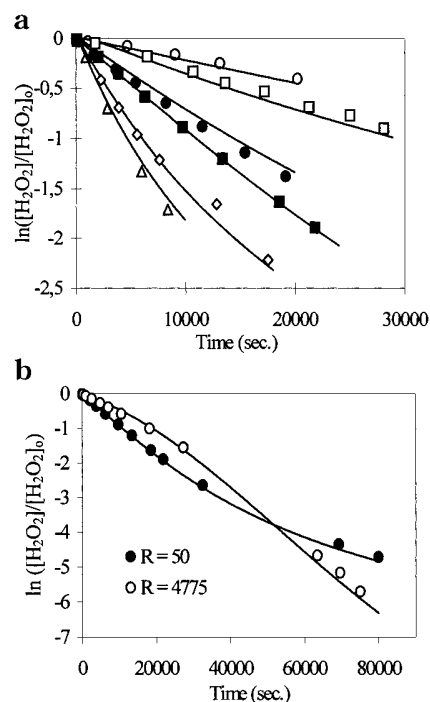


FIGURE 3. Predicted (solid lines) and experimental (symbols) concentration-time profiles for H_2O_2 at $\text{pH} 3.0$ (25°C ; $I = 0.1\ \text{M}$; $R = [\text{H}_2\text{O}_2]_0/[\text{Fe(III)}]_0$): (a) experiment nos. 1 (\circ), 4 (\bullet), 7 (\diamond), 8 (\triangle), 10 (\square), 12 (\blacksquare) from Table 4 and (b) effect of $[\text{H}_2\text{O}_2]_0/[\text{Fe(III)}]_0$; $[\text{Fe(III)}]_0 = 200\ \mu\text{M}$.

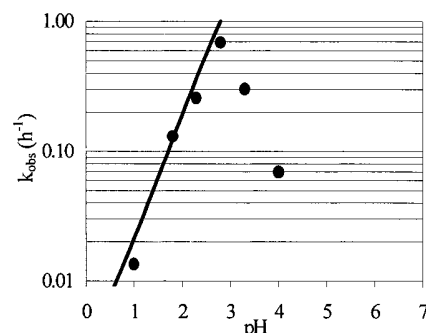


FIGURE 4. Comparison of k_{obs} values predicted by our kinetic model (solid lines) with the experimental values (symbols) obtained by Pignatello (40) ($[\text{Fe(III)}]_0 = 0.99\ \text{mM}$; $[\text{H}_2\text{O}_2]_0 = 0.1\ \text{M}$; 25°C ; $I = 0.2\ \text{M NaClO}_4$). Computation has been made by using the following values: $K_1 = 2.44 \times 10^{-3}\ \text{M}$; $K_2 = 6.47 \times 10^{-7}\ \text{M}$; $K_{I1} = 2.40 \times 10^{-3}$; and $K_{I2} = 1.6 \times 10^{-4}$, $\gamma_{\text{H}^+} = 0.75$.

complex kinetic rates have not been incorporated in the model. It should also be noted that the pseudo-first-order rate constants determined by Pignatello (40) at various pH could also be calculated by our kinetic model after correcting the equilibrium constants for the experimental conditions used by the author (Figure 4).

Furthermore, the decay of absorbance in the region $300\text{--}550\ \text{nm}$ with reaction time could also successfully be predicted by our kinetic model by using the molar absorptivities of Fe(III) -hydroxy complexes and Fe(III) -hydroperoxy complexes reported in a previous paper (22) (Figure 5).

Discussion

Distribution of Fe(III) Species in Homogeneous Aqueous Solution. According to the reaction scheme presented in Table 2, the mechanism of decomposition of H_2O_2 by Fe(III)

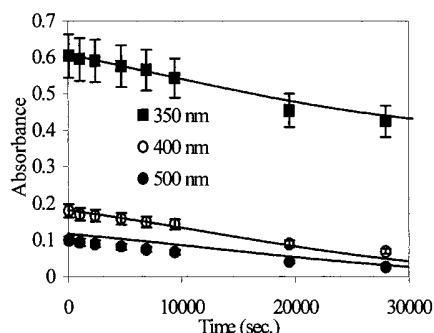


FIGURE 5. Comparison of measured (symbols) and computed values (solid lines) of the absorbances at 350, 400, and 500 nm of the solution versus reaction time (pH = 3.0; $[\text{Fe(III)}]_0 = 200 \mu\text{M}$; $[\text{H}_2\text{O}_2]_0 = 1 \text{ M}$; optical path length 5 cm; 25.0 °C; $I = 0.1 \text{ M}$).

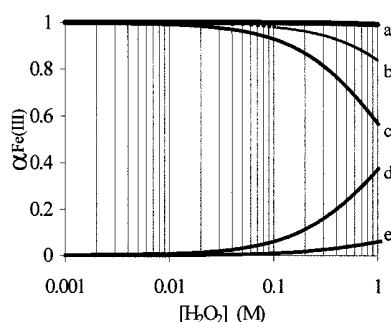


FIGURE 6. Effect of hydrogen peroxide concentration on the distribution of uncomplexed Fe(III) ($\alpha_{\text{Fe(III)}}$) at pH 1.0 (a), 2.0 (b), and 3.0 (c) and of Fe(III)–peroxy complexes α_{I1} (d) and α_{I2} (e) at pH 3.0 ($[\text{Fe(III)}]_T = 200 \mu\text{M}$; 25 °C; $I = 0.1 \text{ M}$).

is initiated by the unimolecular decomposition of Fe(III)–hydroperoxy complexes I_1 and I_2 (reactions II.6a and II.6b in Table 2). It has been assumed that propagation and termination reactions only involve Fe(II) and uncomplexed Fe(III).

Assuming that (i) $[\text{Fe}^{2+}] \ll [\text{Fe(III)}]_T$ and (ii) the concentration of the dimer in eq 12 can be neglected, the fraction of Fe(III) present in the form of uncomplexed Fe(III) ($\alpha_{\text{Fe(III)}}$) and of complexed Fe(III) ($\alpha_{\text{I1}} + \alpha_{\text{I2}}$) can be expressed as

$$\alpha_{\text{Fe(III)}} = \frac{[\text{Fe(III)}]}{[\text{Fe(III)}]_0} = \frac{[\text{H}^+]^2 + K_1[\text{H}^+] + K_2}{[\text{H}^+]^2 + K_1[\text{H}^+] + K_2 + [\text{H}_2\text{O}_2](K_{\text{I1}}[\text{H}^+] + K_{\text{I1}}K_{\text{I2}})} \quad (15)$$

$$\alpha_{\text{I1}} + \alpha_{\text{I2}} = 1 - \alpha_{\text{Fe(III)}} \quad (16)$$

Equations 15 and 16 indicate that $\alpha_{\text{Fe(III)}}$, α_{I1} , and α_{I2} depend only on pH and on the concentration of H_2O_2 . In Figure 6, $\alpha_{\text{Fe(III)}}$ is plotted as a function of $[\text{H}_2\text{O}_2]$ for pH 1, 2, and 3. Figure 6 illustrates that the fraction of Fe(III) present in the form of Fe(III)–peroxy complexes is very small at pH 1 ($\alpha_{\text{Fe(III)}} > 0.99$) and becomes significant at concentrations of H_2O_2 higher than 0.1 M at pH 3.0.

Apparent Second-Order Rate Constant for the Initiation Step. Assuming that I_1 and I_2 are in a very fast equilibrium with Fe(III) and H_2O_2 , the rate of the initiation step of the mechanism of decomposition of H_2O_2 by Fe(III) can be written as

$$d[\text{Fe}^{2+}]/dt = k_6([\text{I}_1] + [\text{I}_2]) \quad (17)$$

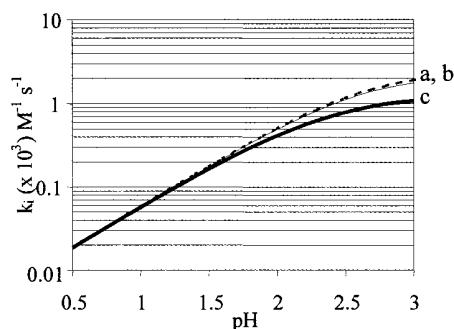


FIGURE 7. Effect of pH and $[\text{H}_2\text{O}_2]$ ((a) $[\text{H}_2\text{O}_2] = 1 \text{ mM}$; (b) $[\text{H}_2\text{O}_2] = 0.1 \text{ M}$; and (c) $[\text{H}_2\text{O}_2] = 1 \text{ M}$) on the pseudo-second-order rate constant (k_i) of the initiation step of the mechanism of H_2O_2 decomposition by Fe(III) ($[\text{Fe(III)}]_0 = 200 \mu\text{M}$; 25.0 °C; $I = 0.1 \text{ M}$).

By considering the equilibrium constants K_{I1} and K_{I2} , eq 17 becomes

$$\frac{d[\text{Fe}^{2+}]}{dt} = k_6 \left(\frac{K_{\text{I1}}}{[\text{H}^+]} + \frac{K_{\text{I1}}K_{\text{I2}}}{[\text{H}^+]^2} \right) [\text{Fe}^{3+}][\text{H}_2\text{O}_2] \quad (18)$$

By introducing $\alpha_{\text{Fe(III)}}$ into eq 18, the following expression for the rate of the initiation step can be derived

$$\frac{d[\text{Fe}^{2+}]}{dt} = k_i [\text{Fe(III)}]_0 [\text{H}_2\text{O}_2] \quad (19)$$

where k_i is the apparent second-order rate constant for the initiation step of the mechanism of decomposition of H_2O_2 by Fe(III):

$$k_i = \frac{k_6(K_{\text{I1}}[\text{H}^+] + K_{\text{I1}}K_{\text{I2}})}{[\text{H}^+]^2 + K_1[\text{H}^+] + K_2} \alpha_{\text{Fe(III)}} \quad (20)$$

Since $\alpha_{\text{Fe(III)}}$ depends on the concentration of Fe(III), H_2O_2 , and of pH, k_i is not constant. Using the equilibrium constants listed in Table 2, k_i has been plotted as a function of pH in Figure 7 for three concentrations of H_2O_2 (0.001, 0.1, and 1 M) and for $[\text{Fe(III)}]_0 = 200 \mu\text{M}$. As Figure 7 illustrates, k_i increases with pH (pH 1.0: $k_i = 6.9 \times 10^{-5} \text{ M}^{-1} \text{ s}^{-1}$; pH 2.0: $k_i = 5.6 \times 10^{-4} \text{ M}^{-1} \text{ s}^{-1}$; pH 3: $k_i = 1.9 \times 10^{-3} \text{ M}^{-1} \text{ s}^{-1}$, values calculated for $[\text{H}_2\text{O}_2] < 0.1 \text{ M}$). Concentration of H_2O_2 has a significant effect on the value of k_i at pH > 2.0 (at pH = 3.0: $k_i = 1.9 \times 10^{-3} \text{ M}^{-1} \text{ s}^{-1}$ for $[\text{H}_2\text{O}_2] = 0.1 \text{ M}$; $1.2 \times 10^{-3} \text{ M}^{-1} \text{ s}^{-1}$ for $[\text{H}_2\text{O}_2] = 1 \text{ M}$).

Effect of $[\text{H}_2\text{O}_2]_0/[\text{Fe(III)}]_0$ on k_{obs} at pH 3.0. At pH 3.0, experimental and simulated data have shown that the pseudo-first-order kinetic constant for the initial rate of decomposition of H_2O_2 depends on the ratio of concentrations of H_2O_2 to Fe(III) (Figure 2) and that the overall decomposition rate of H_2O_2 deviates from a first-order kinetic law during the course of the reaction. As pointed out by Barb et al. (16) and Walling and Weil (17), the steady-state concentration of Fe(II) plays a key role in the rate of decomposition of H_2O_2 .

To illustrate the effect of $[\text{H}_2\text{O}_2]_0/[\text{Fe(III)}]_0$ on the concentration of Fe(II), the kinetic model was used to calculate concentration–time profiles for Fe(II) for the experiments conducted at pH 3.0 and with $[\text{Fe(III)}]_0 = 200 \mu\text{M}$. Figure 8 shows that Fe(II) concentration versus reaction time reaches a maximum value and that its maximum concentration depends on $[\text{H}_2\text{O}_2]_0/[\text{Fe(III)}]_0$.

For $[\text{H}_2\text{O}_2]_0/[\text{Fe(III)}]_0$ values lower than 50, an increase of the initial concentration of H_2O_2 enhances the initial rate of formation of Fe(II) and leads to an increase of the concentration of Fe(II) in the solution. Once formed, Fe(II) may be

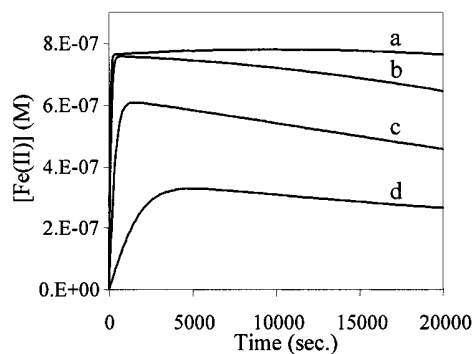


FIGURE 8. Simulated concentration–time profiles of Fe(II) for various ratios $[H_2O_2]_0/[Fe(III)]_0$ (R) and for reaction time corresponding to the determination of k_{obs} ($t < 20\,000$ s; $[Fe(III)]_0 = 200\ \mu M$; (a) $R = 250$; (b) $R = 50$; (c) $R = 10$; (d) $R = 1$; pH 3.0; 25 °C; $I = 0.1$ M).

oxidized by $\cdot OH$ to yield Fe(III) or may further promote the decomposition of H_2O_2 . By considering these two reactions, increasing H_2O_2 concentration will accelerate the rate of decomposition of H_2O_2 . This is consistent with the experimental data.

For $50 < [H_2O_2]_0/[Fe(III)]_0 < 500$, most of the OH radicals are scavenged by H_2O_2 ($k_9[H_2O_2] \gg k_8[Fe(II)]$). Consequently, reaction II.8 in Table 2 can be ignored. By assuming that reactions II.13a–II.15 in Table 2 are also of little importance, the following simplified expression for the overall decomposition rate of H_2O_2 can be derived:

$$-d[H_2O_2]/dt = 2k_7[Fe^{2+}]_{ss}[H_2O_2] = k_{obs}[H_2O_2] \quad (21)$$

The steady-state concentration of Fe^{2+} is defined by

$$[Fe^{2+}]_{ss} = \left(\frac{k_i k_{11app}}{k_7 k_{10app}} \right)^{1/2} [Fe(III)]_0 \quad (22)$$

where k_i is given by eq 20. k_{10app} and k_{11app} are the apparent second-order rate constants of $HO_2^*/O_2^{\cdot -}$ with Fe(II) (reactions II.10a and II.10b in Table 2) and Fe(III) (reactions II.11a and II.11b in Table 2), respectively (at pH 3: $k_{10app} = 1.3 \times 10^6\ M^{-1}\ s^{-1}$ and $k_{11app} = 6.6 \times 10^5\ M^{-1}\ s^{-1}$).

Expressions 17 and 18 are similar to those formulated by Barb et al. (16), except that the formation and the decomposition of Fe(III)–hydroperoxy complexes have been taken into account in our reaction scheme and incorporated in the expression for k_i (eq 20). Since $\alpha_{Fe(III)}$ and k_i are nearly constant for $[H_2O_2]$ values less than 0.1 M at pH 3 (Figure 7), eq 22 indicates that $[Fe^{2+}]_{ss}$ is not a function of the concentration of H_2O_2 and is linearly dependent upon $[Fe(III)]_0$. Therefore, k_{obs} will be constant and the overall decomposition of H_2O_2 will be second-order:

$$-\frac{d[H_2O_2]}{dt} = k_d[Fe(III)][H_2O_2] \quad (23)$$

with $[Fe(III)] \approx [Fe(III)]_0$ and

$$k_d = \left(\frac{k_i k_7 k_{11app}}{k_{10app}} \right)^{1/2} \quad (24)$$

Under conditions stated above ($50 < [H_2O_2]_0/[Fe(III)]_0 < 500$, pH 3.0), computed concentration–time profiles for Fe^{2+} confirm that Fe^{2+} concentration rapidly reaches a “plateau” which is independent of $[H_2O_2]$ and proportional to $[Fe(III)]_0$. Furthermore with Fe(II) concentration at its maximum, k_{obs} or k_d values calculated from the kinetic model were consistent with those given by eqs 21 and 24, respectively. The difference between computed and calculated values was

less than 10% and can be attributed to the uncertainties on the measured values of pH and k_{obs} .

For $[H_2O_2]_0/[Fe(III)]_0$ values above 500 at pH 3, the decrease of k_{obs} with increasing $[H_2O_2]_0/[Fe(III)]_0$ (Figure 2a) can be explained by the fact that the fraction of Fe(III) present in the form of Fe(III)–hydroperoxy complexes becomes significant at pH 3.0. Under these experimental conditions, $\alpha_{Fe(III)}$ decreases when $[H_2O_2]_0/[Fe(III)]_0$ increases (Figure 6), and as expected from eqs 20 and 24, the overall decomposition rate of H_2O_2 will decrease.

It should be noted that at pH < 3 , the effect of $[H_2O_2]_0/[Fe(III)]_0$ on $\alpha_{Fe(III)}$ should be less important. As is shown in Figure 6, $\alpha_{Fe(III)}$ is close to 1.0 for $[H_2O_2] < 0.1$ M at pH 1 and 2; model prediction as well as experimental data did not show a decrease of k_{obs} .

Deviation from the Pseudo-First-Order Kinetics. During the course of the reaction, the ratio of concentration of H_2O_2 to Fe(III) ($[H_2O_2]/[Fe(III)]$, $[Fe(III)] \approx [Fe(III)]_0$) decreases. Since k_{obs} is a function of $[H_2O_2]_0/[Fe(III)]_0$ (Figure 2a), the slope of $\ln([H_2O_2]/[H_2O_2]_0) = f(t)$ will not be constant, and the rate of decomposition of H_2O_2 will deviate from the pseudo-first-order kinetic law. This is in good agreement with our experimental and simulated data (Figure 3b). For the experiment carried out at pH 3.0 and with $[H_2O_2]_0/[Fe(III)]_0 = 4775$, the slope of $\ln([H_2O_2]/[H_2O_2]_0)$ versus reaction time increases during the course of the reaction until $[H_2O_2]/[Fe(III)]$ becomes lower than 500. On the other hand, a decrease of the slope of $\ln([H_2O_2]/[H_2O_2]_0) = f(t)$ can be observed when $[H_2O_2]/[Fe(III)]$ becomes lower than 50.

The results of this study show that our model adequately simulates the complex kinetics of decomposition of H_2O_2 by Fe(III) in homogeneous aqueous solution. Nevertheless, the model can only be used for reactions conducted in $HClO_4$ / $NaClO_4$ solutions since the presence of other inorganic anions (chloride, sulfate, ...) might have a significant effect on the distribution of ferric complexes and therefore on the overall rate of decomposition of H_2O_2 .

Literature Cited

- (1) Fenton, H. J. H. *J. Chem. Soc.* **1894**, 65, 899.
- (2) Haber, F.; Weiss, J. *Proc. Roy. Soc. A* **1934**, 134, 332–351.
- (3) Barb, W. G.; Baxendale, J. H.; George, P.; Hargrave, K. R. *Nature* **1949**, 163, 692–694.
- (4) Kremer, M. L.; Stein, G. *Trans. Faraday Soc.* **1959**, 55, 959–973.
- (5) Walling, C.; Cleary, M. *Int. J. Chem. Kinet.* **1977**, 9, 595–601.
- (6) Cohen, G.; Sinet, P. M. *Dev. Biochem.* **1980**, 11, 27–37.
- (7) Sawyer, D. T.; Kang, C.; Llobet, A.; Redman, C. J. *Am. Chem. Soc.* **1993**, 115, 5817–5818.
- (8) Graedel, T. E.; Mandich, M. L.; Weschler, C. J. *J. Geophys. Res.* **1986**, 91, 4, 5205–5221.
- (9) Sedlak, D. L.; Hoigne, J. *Environ. Sci. Technol.* **1994**, 28, 11, 1898–1906.
- (10) Voelker, B. M.; Morel, F. M. M.; Sulzberger, B. *Environ. Sci. Technol.* **1996**, 30, 1106–1114.
- (11) Eisenhauer, H. R. J. *Water Pollut. Control Fed.* **1964**, 36, 9, 1116–1128.
- (12) Murphy, A. P.; Boegli, W. J.; Price, M. K.; Moody, C. D. *Environ. Sci. Technol.* **1989**, 23, 2, 166–169.
- (13) Safarzadeh-Amiri, A.; Bolton, J. R.; Cater, S. R. *J. Adv. Oxid. Technol.* **1996**, 1, 1, 18–26.
- (14) Pignatello, J. J.; Huang, L. Q. *Water Res.* **1993**, 27, 12, 1731–1736.
- (15) Mazellier, P.; Jirkovsky, J.; Bolte, M. *Pestic. Sci.* **1997**, 49, 259–267.
- (16) Barb, W. G.; Baxendale, J. H.; George, P.; Hargrave, K. R. *Trans. Faraday Soc.* **1951**, 47, 591–616.
- (17) Walling, C.; Weil, T. *Int. J. Chem. Kinet.* **1974**, 6, 507–516.
- (18) Evans, M. G.; George, P.; Uri, N. *Trans. Faraday Soc.* **1949**, 45, 230–236.
- (19) Jones, P.; Kitching, R.; Tobe, M. L.; Wynne-Jones, W. F. K. *Trans. Faraday Soc.* **1959**, 55, 79–90.
- (20) Haggitt, M. L.; Jones, P.; Wynne-Jones, W. F. K. *Discuss. Faraday Soc.* **1960**, 29, 153–162.
- (21) Lewis, T. J.; Richards, D. H.; Salt, D. A. *J. Chem. Soc.* **1963**, 2434–2442.

- (22) Gallard, H.; De Laat, J.; Legube, B. *Water Res.* In press.
- (23) Walling, C.; Goosen, A. J. *Am. Chem. Soc.* **1973**, 95, 9, 2987–2991.
- (24) Kremer, M. L.; Stein, G. *Int. J. Chem. Kinet.* **1977**, 9, 179–184.
- (25) Milburn, R. M.; Vosburgh, W. C. *J. Am. Chem. Soc.* **1955**, 77, 1352–1355.
- (26) Knight, R. J.; Sylva, R. N. *J. Inorg. Nucl. Chem.* **1975**, 37, 779–783.
- (27) Gallard, H.; De Laat, J.; Legube, B. *New J. Chem.* **1998**, 263–268.
- (28) Goldstein, S.; Czapski, G.; Meyerstein, D. *Free Radicals Biol. Med.* **1993**, 15, 435–445.
- (29) Sychev, A. Y.; Isaak, V. G. *Russ. Chem. Rev.* **1995**, 64, 1105–1129.
- (30) Bossmann, S. H.; Oliveros, E.; Göb, S.; Siegwart, S.; Dahlen, E. P.; Payawan, L.; Straub, M.; Wörner, M.; Braun, A. M. *J. Phys. Chem. A* **1998**, 102, 5542–5550.
- (31) Stuglik, Z.; Zagorski, Z. P. *Radiat. Phys. Chem.* **1981**, 17, 229–233.
- (32) Christensen, H.; Sehested, K.; Corfitzen, H. J. *Phys. Chem.* **1982**, 86, 1588–1590.
- (33) Jayson, G. G.; Parsons, B. J.; Swallow, A. J. *J. Chem. Soc., Faraday Trans I* **1973**, 69, 236–242.
- (34) Rush, J. D.; Bielski, B. H. J. *J. Phys. Chem.* **1985**, 89, 23, 5062–5066.
- (35) Rothschild, W. G.; Allen, A. O. *Radiat. Res.* **1958**, 8, 101–110.
- (36) Bielski, B. H. J.; Cabelli, D. E.; Arudi, R. L.; Ross, A. B. *J. Phys. Chem. Ref. Data* **1985**, 14, 4, 1041–1100.
- (37) Sehested, K.; Rasmussen, O. L.; Fricke, H. J. *Phys. Chem.* **1968**, 72, 2, 626–631.
- (38) *Eaux méthodes d'essai – recueil de normes françaises*, 4th ed; AFNOR, ISBN 2-12-179041-1, 1990.
- (39) Eisenberg, G. M. *Ind. Eng. Chem.* **1943**, 15, 5, 327–328.
- (40) Pignatello, J. J. *Environ. Sci. Technol.* **1992**, 26, 5, 944–951.

Received for review November 12, 1998. Revised manuscript received March 7, 1999. Accepted March 10, 1999.

ES981171V